Design, Synthesis, and Conformational Analysis of a Novel Macrocyclic HIV-Protease Inhibitor

Brent L. Podlogar,* Robert A. Farr, Dirk Friedrich, Celine Tarnus, Edward W. Huber, Robert J. Cregge, and Daniel Schirlin

Marion Merrell Dow Research Institute, 2110 East Galbraith Road, Cincinnati, Ohio 45215-6300, and Marion Merrell Dow Strasbourg Research Center, 16 rue d'Ankara, 67046 Strasbourg Cedex, France

Received March 9, 1994®

Design modifications to the lead HIV-PR inhibitor **1** (MDL 73,669, K_i = 5 nM) have been postulated based on a computational model of the **1**/HIV-PR complex. A novel macrocyclic inhibitor **8** (MDL 104,168) wherein the P_1 and P_3 side chains of the original acyclic inhibitor have been joined retains good biological activity (K_i = 20 nM). NMR analysis of the precursor alcohol (*S*)-**7** shows the conformation of the cyclic region to be very similar to that observed in the enzyme-bound **8** as determined by the computational model. Consistency of the computational model with NMR data and in vacuo molecular dynamics simulations provide the basis for postulating further modifications of the cyclic inhibitor expected to optimize its interactions with HIV-PR.

Introduction

Recently, Schirlin and co-workers have reported details of 1 (MDL 73,669), an HIV-PR inhibitor containing a difluorostatone peptide mimetic,[1a] which exhibits remarkable in vitro inhibition (K_i = 5 nM).[1b] As a part of our efforts to improve the selectivity index of this lead compound, we have developed a structural model of the 1/HIV-PR complex to examine the interactions between the ligand and the enzyme at the atomic level. During the course of these studies, we discovered that cyclic variants possessing covalently linked P_1 and P_3 side chains qualify as potential inhibitors and have subsequently verified that they in fact retain biological activity. Incorporation of a cyclic constraint is believed to hold potential for further development toward improved and ultimately non-peptidic HIV-PR inhibitors.[2] The details of the design process, synthesis, and conformational analysis are reported herein.

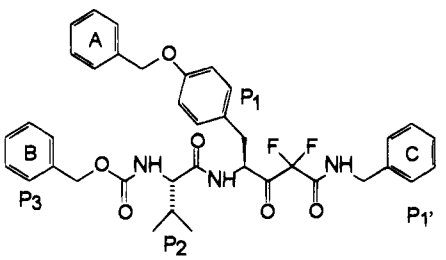

1, MDL 73,669

Results and Discussion

We targeted modifications of **1** that would remain within the established synthetic framework of the difluorostatone amide bond surrogate but would also address one or all of the following attributes: (a) increased affinity through additional favorable interactions with the active site of HIV-PR, e.g., H bonds, electrostatic interactions; (b) decreased overall molecular weight by eliminating portions not vital to the recognition and binding process; (c) introduction of conformational constraints that render the solution conformation similar to the bound conformation. Since no structural data on the **1**/HIV-PR complex was available in the initial stages of this work, it was necessary to construct a suitable structural model to guide in the design process.

Molecular Modeling. The crystal structures of free HIV-PR[3] and of its co-crystallization complexes with the reduced inhibitor MVT-101,[4] the hydroxyethylamine inhibitor JG-365,[5] and acetyl-pepstatin,[6] as well as others,[7] have been solved to atomic resolution and are available in the Brookhaven Protein Database.[8] These X-ray structures accurately describe the conformations of the various inhibitors as they exist *in the act of inhibiting* HIV-PR, the so-called bound conformations, and simultaneously provide information about the preferred conformations of the protease *as it is being inhibited*. This information constituted the basis for the development of the structural models used in our studies. The rms deviations between the coordinates of HIV-PR in the different complexes are well within the experimental resolution of the individual determinations regardless of which ligand occupies the active site. On the basis of this observation, potential inhibitors not already synthesized might be *computationally co-crystallized* by simply fitting the inhibitor of interest into the empty active site and abating any small van der Waals interactions via molecular mechanics (MM) and molecular dynamics (MD) calculations. This protocol was applied to **1**, and full details for the construction of the 1/HIV-PR complex model are described in the Experimental Section. Because of their close structural similarities, any of the available co-crystallization complexes could be used for the construction of the 1/HIV-PR model. We have chosen the atomic coordinates of HIV-PR derived from its co-crystallization complex with MVT-101.[4]

The HIV-PR portion of the model 1/HIV-PR complex (Figure 1) is consistent with the published X-ray structures and is therefore considered a valid basis for the inhibitor design process. The rms deviations between the protease backbone coordinates derived from the

* Author to whom correspondence should be sent. Current address: R. W. Johnson Pharmaceutical Research Institute. Route 202, P.O. Box 300, Raritan, NJ 08869.

® Abstract published in *Advance ACS Abstracts*, September 15, 1994.

0022-2623/94/1837-3684$04.50/0

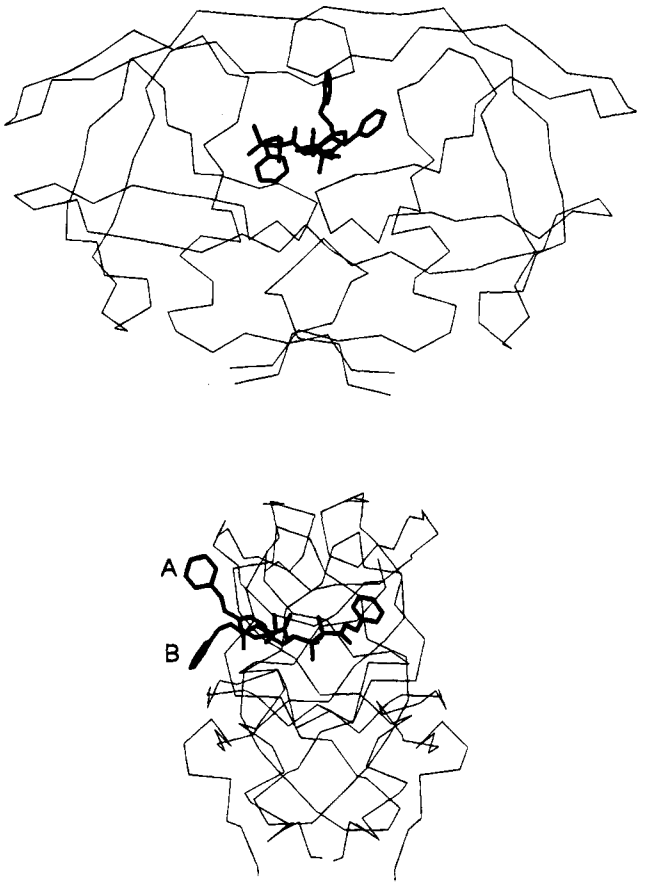

Figure 1. Orthogonal views of the 1/HIV-PR model. Phenyl rings A and B project out of the active site cavity and into the solvent medium.

model and those provided by the X-ray structures are on average less than 1.0 Å. Regions of high flexibility as determined by MD are in fact seen to exhibit larger crystallographic *B* factors in the published X-ray structures, particularly near the entrance of the active site and in the loop regions.

Drug Design. The model in Figure 1 clearly shows that phenyl rings A and B of **1** project out of the active site and into the solvent medium, thus creating an unfavorable hydrophobic–hydrophilic interface. Accordingly, consideration was given to removing ring A outright and replacing ring B with another, more hydrophilic group. Preliminary SAR studies indicated, however, that the presence of ring A decreases the inhibitor's cytotoxicity.[1b] The steric bulk that ring A offers may therefore be crucial for ensuring selectivity for the HIV-PR. Analysis of the MD simulation performed in the refinement protocol of the 1/HIV-PR complex model shows rings A and B to be in close contact throughout the simulation, either as a result of a $\pi-\pi$ interaction or perhaps symptomatic of hydrophobic collapse.[9] The diminished dynamical motion of rings A and B was considered significant since the "arms" on which they are attached join into the inhibitor adjacent to the difluorostatone functionality which in turn interacts directly with the enzyme active site. Their decreased mobility may translate into a predisposition for the bioactive conformation in the active-site region that would be lost upon the removal of either of the rings A or B.

Consequently, we postulated that elimination of the hydrophobic phenyl rings A and B and simultaneous

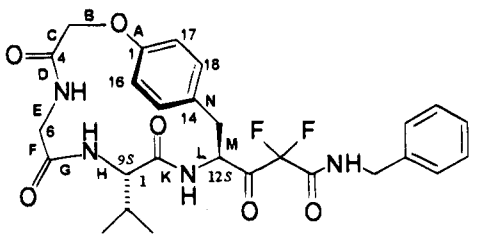

Figure 2. The macrocyclic framework shown for inhibitor **8**. Shown also is the numbering scheme and dihedral angle designations.

introduction of a conformational constraint could be achieved by linking the P_1 and P_3 residues. A P_1/P_3 linkage has been suggested for other aspartic protease inhibitors.[10] Logical extension of this strategy to the present system could be easily attained with great design variability by replacing the P_3 protecting group with a suitably protected amino acid via standard coupling procedures. Retrosynthetic analysis suggests that deprotection of the *N*-terminal amine could lead to spontaneous cyclization onto the P_1 subsite by reaction with an activated ester functionality appropriately amended onto the P_1 tyrosyl hydroxyl group. The framework of such a potential cyclic inhibitor is represented by ketone **8** in Figure 2. Manipulating the nature and relative stereochemistry of substituents at C-6 would provide a means for modulating steric bulk and conformational preference in the macrocyclic region of the molecule and for increasing interactions with appropriate residues of HIV-PR (vide infra).

The proposed macrocyclic inhibitor exhibits many of the targeted features: (1) the undesired hydrophobic–hydrophilic gradient presumed unnecessary for binding has been decreased by removal of phenyl rings A and B, (2) the overall molecular weight has been decreased, and (3) a conformational constraint has been introduced. For a final a priori evaluation, the parent macrocycle **8** was docked into the active site of the HIV-PR in a similar manner as described for **1**. Small van der Waals contacts with the HIV-PR were eliminated by the MD protocol described in the Experimental Section. Figure 3 shows the bound conformations of **1** and **8**. We were pleased to find that these modifications could be accommodated according to our a priori modeling studies and proceeded to synthesize the proposed inhibitor.[11]

Inhibitor Synthesis and Biological Activity. The synthetic route to macrocyclic inhibitor **8** is summarized in Scheme 1. Ether **2**,[1] a 6:1 mixture of diastereomers with the (*R*)-alcohol predominating,[12] was debenzylated with palladium black in 4.4% HCO_2H/CH_3OH[13] to give phenol **3**. Alkylation of phenol **3** with ethyl bromoacetate/K_2CO_3 and catalytic KI in acetone afforded ether **4**. The site of alkylation was verified by ^1H NMR: the phenolic O**H** and the amide N**H**CH_2Ph protons of phenol **3**, which overlap at δ 9.17 as a narrow multiplet, are replaced by a single proton multiplet at δ 9.19 in the ^1H NMR of ether **4**. Irradiation at δ 9.19 collapsed the N**H**CH_2Ph protons to doublets, while irradiation at δ 3.94, the common chemical shift for both methine protons, collapsed the Boc**NH** and alcohol O**H** from doublets to singlets. Standard deprotection and coupling with Boc-Gly-Val gave methyl ester **5**, which was subsequently converted to the activated pentafluoro-

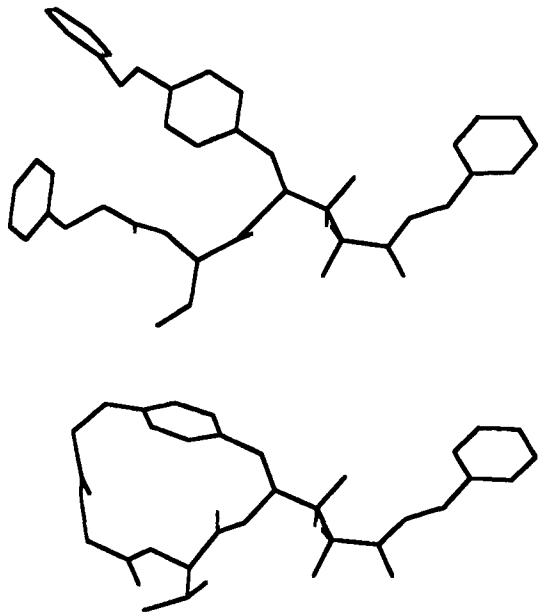

Figure 3. The bound conformations of 1 (top) and **8**.

phenyl ester **6**. Removal of the *N*-Boc protecting group from ester **6** with 4 N HCl/dioxane and treatment of the resulting amine hydrochloride salt with aqueous $NaHCO_3/CH_2Cl_2$ gave the macrocyclic alcohol **7**.[14] The macrocyclic alcohol **7** was readily separated from less soluble polymeric material by repeated trituration with hot $EtOAc/CF_3CH_2OH$ followed by filtration; concentration of the filtrate gave pure 16-membered ring alcohol **7** in 51–79% yield. Swern oxidation gave a mixture of products, from which we were able to separate, in very low yield, ketone **8**. In contrast, the oxidation of alcohol (*S*)-**7** using 5 equiv of the Dess–Martin periodinane[15] for 4 days gave an approximate 2:2:1 mixture of recovered (*S*)-**7**/**8**/**8**·H_2O.[16] Addition of water to a DMSO-d_6 solution of the mixture gave a 4:1:5 mixture, respectively, after 1.5 h.

The biological activity was assessed using an enzyme assay previously defined;[17–19] **8** possessed a K_i of 20 nM.

NMR Analysis of the Cyclic Inhibitor. We were particularly interested to note whether the macrocyclic portion of **8** would, in free solution, resemble the bound conformation as defined by the **8**/HIV-PR complex model. Because of the limited quantity of ketone **8**, we elected to subject alcohol (*S*)-**7** to a detailed NMR analysis. This substitution appeared acceptable, because the macrocyclic portion in which we were most interested should behave in a similar fashion for both **7** and **8**, particularly when considering that the ketone functionality of **8** is probably hydrated to an sp^3 center in the active species.[20]

All proton resonances of (*S*)-**7** (500 MHz, DMSO-d_6, 20 °C) are sharp, indicating either a unique solution conformation or interconversion between different conformations at a rate that is fast on the time scales defined by associated chemical shift variations.[21] The spectrum is well-dispersed and could be readily assigned from a DQF-COSY spectrum. All homonuclear coupling constants could be directly extracted from the 1D spectrum. In a variable-temperature study (400 MHz, 20–85 °C), all exchangeable protons experienced monotonous upfield shifts with increasing temperature, thus giving no indication of profound conformational changes in this temperature range. Significantly smaller temperature coefficients observed for the glycine and valine NH protons (H-5 and H-8) indicated their being, on average, less exposed to solvation as a result of some degree of internal orientation.[22]

The ^{19}F NMR spectrum showed a pair of sharp, geminally coupled resonances, which were further split by vicinal ^1H, ^{19}F coupling. The ^{13}C NMR spectrum could be fully assigned based on chemical shifts, observed ^{13}C, ^{19}F coupling, a HETCOR spectrum, and selective DEPT-45 spectra[23] for correlation, via $^2J_{C,H}$, of the amide carbonyls with adjacent amide protons.

NOESY spectra of (*S*)-**7** showed all observable NOEs to be negative with the exception of those correlations involving the side chain phenyl and methyl groups, which obviously enjoy additional degrees of motional freedom relative to the macrocyclic core. Deserving comment is an exceptional correlation observed between H-15 and H-18, which was recognized as due to chemical exchange by observation of a corresponding negative correlation in a ROESY spectrum. Analogous correlations for the H-16, H-17 pair could not be discerned due to their small shift difference. This exchange phenomenon is obviously caused by a 180° flip of the *p*-phenylene ring occurring at a rate that is slow compared to the smallest involved shift difference, namely $\Delta\delta$ = 37 Hz between H-16 and H-17. An upper limit for the frequency of this flip can be estimated as $k \ll 2\pi\Delta\delta$ = ca. 230 Hz,[21] but a considerably slower frequency is indicated by the fact that the four aromatic protons involved were nevertheless showing distinctly different patterns of genuine NOEs at mixing times up to 1000 ms.

Comparison of NOESY data obtained at several mixing times in the range of 150–1000 ms showed no indication for significant buildup of indirect correlations. It thus appeared permissible to base a qualitative interpretation on a classification of the conformationally relevant NOEs into categories of strong, medium, weak, and absent by evaluation of the NOESY spectrum obtained at the shortest mixing time of 150 ms. These assignments, as well as the relevant vicinal coupling constants, are summarized in Table 1 together with conservative estimates of compatible dihedral angle limits. The following discussion refers to Table 1 and Figure 2.

Observation of sequential $NH^{(i)}$, $H_\alpha^{(i+1)}$ NOEs in the absence of any sequential $H_\alpha^{(i)}$, $H_\alpha^{(i+1)}$ NOEs defines all amide bonds to be (*E*)-configured. The extreme values of the vicinal coupling constants across bonds H, L, and M are only compatible with narrow ranges for the corresponding dihedral angles and are thus indicative of a single principle conformation in this region of the molecule. The observed pattern of NOEs is consistent with this conclusion and extends the conformationally well-defined region over the entire sequence of bonds F–N. For example, observation of strong H-15/H-13$_\beta$ and medium H-18/H-13$_\alpha$ correlations in the absence of H-18/H-13$_\beta$ and H-15/H-13$_\alpha$ correlations confines angle N to the fairly narrow range of $-15° \pm 30°$. Also in line with these assignments are the small temperature coefficient for H-8 mentioned above and the significant upfield shift observed for H-8 which, upon application of the listed dihedral angle constraints to a molecular model, becomes positioned in the shielding area of the *p*-phenylene ring.

Scheme 1[a]

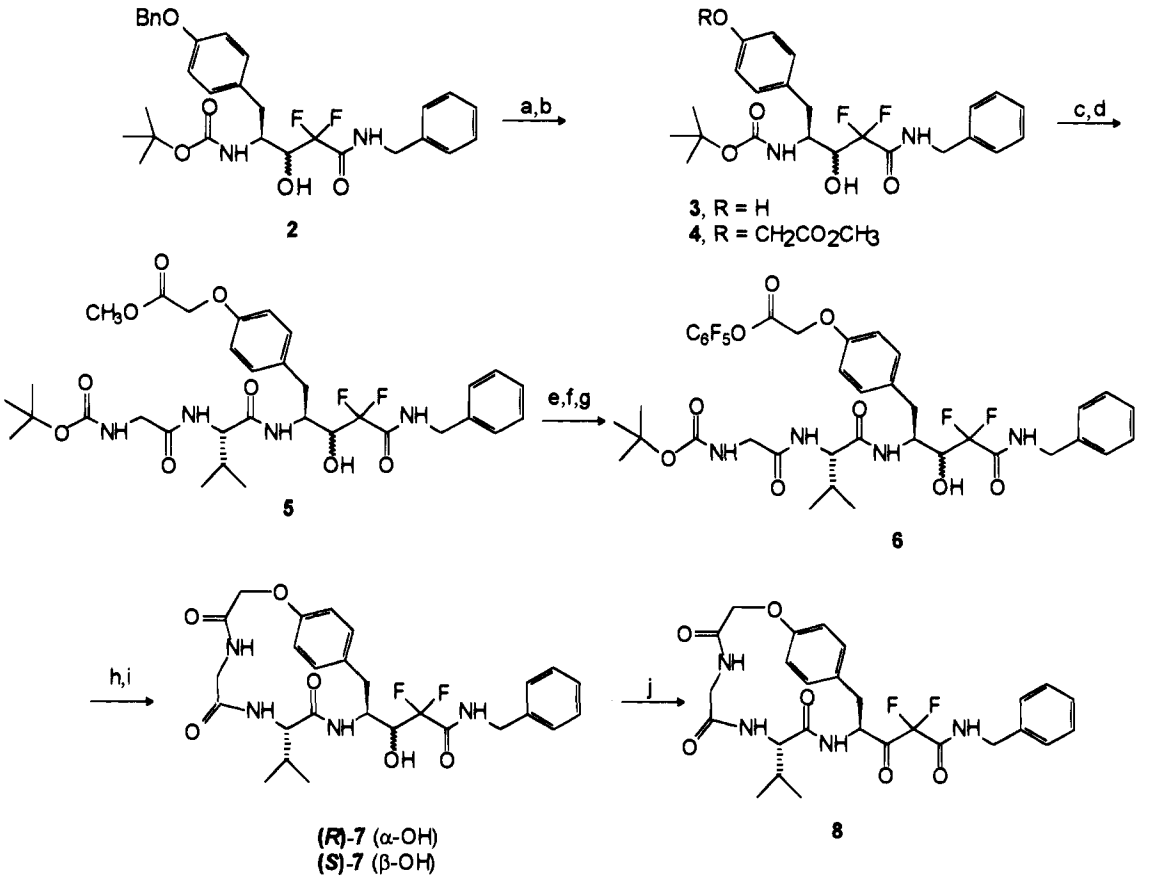

[a] Key: (a) Pd black, 4.4% HCO_2H in CH_3OH; (b) K_2CO_3, cat. KI, $BrCH_2CO_2Et$, acetone; (c) TFA; (d) Boc-Gly-Val, HOBT, EDC; (e) LiOH, CH_3OH/H_2O; (f) $KHSO_4$; (g) C_6F_5OH, EDC; (h) 4 N HCl/dioxane; (i) $NaHCO_3$, CH_2Cl_2; (j) $(COCl)_2$, DMSO; Et_3N.

Table 1. Dihedral Angles in Ketone **8** (by MD) and Alcohol (*S*)-**7** (by NMR)[a]

		ketone **8**			alcohol (*S*)-**7**	
			in vacuo[c]			
dihedral angle definition	code	docked[b]	major	minor	NMR[d] estimate	NOE and *J* information[e]
16C–1C–2O–3C	A	−17	−99	−45	ND	
1C–2O–3C–3αH	Bα	−173	−60	−179	ND	W (3α,16), W (3α,17)
1C–2O–3C–3βH	Bβ	60	−176	68	ND	S (3β,16), N (3β,17)
3αH–3C–4C–4O	Cα	32	−147	26	ND	N (3α,6α), N (3α,6β)
3βH–3C–4C–4O	Cβ	166	−34	139	ND	N (3β,6α), N (3β,6β)
4O–4C–5N–5H	D	174	179		~180	W (3α,5), W (3β,5)
5H–5N–6C–6αH	Eα	170	−69	174	ND	M (5,8)
5H–5N–6C–6βH	Eβ	−56	176	−60	ND	W (5,16), N (5,17)
6αH–6C–7C–7O	Fα	−95	−147		180 ± 45	S (6α,8)
6βH–6C–7C–7O	Fβ	25	−33		−60 ± 45	W (6β,8)
7O–7C–8N–8H	G	−179	179		~180	N (6α,9β), N (6β,9β)
8H–8N–9C–9βH	H	162	−173		±155 ± 20	$J(8,9\beta) = 8.0$
9βH–9C–10C–10O	I	172	−178		180 ± 45	S (9β,11)
10O–10C–11N–11H	K	−173	−178		~180	N (9β,12α)
11H–11N–12C–12αH	L	164	−170		180 ± 20	$J(11,12\alpha) = 9.9$; M (11,15), N (11,18)
12αH–12C–13C–13αH	Mα	−59	−67		−60 ± 20	$J(12\alpha,13\alpha) = 3.5$; W (12α,18)
12αH–12C–13C–13βH	Mβ	180	−179		180 ± 20	$J(12\alpha,13\beta) = 12.1$; N (12α,15)
13αH–13C–14C–15C	Nα	−130	−129		−135 ± 30	N (13α,15), M (13α,18), N (13α,11)
13βH–13C–14C–15C	Nβ	−12	−17		−15 ± 30	S (13β,15), N (13β,18), M (13β,11)

[a] Positive values refer to clockwise, negative values to counterclockwise rotation. The α and β designations refer to Figure 2, α indicating below plane and β indicating above plane hydrogens. [b] Angles representing the minimized structure of the **8**/HIV-PR complex model. [c] Angles representing time averages of the values assumed over the course of the simulation. [d] Angles based on *J* information where available, on NOE information otherwise. [e] *J* values in hertz; NOEs are classified as strong (S), medium (M), weak (W), and absent (N) based on qualitative evaluation of a NOESY spectrum recorded with 150 ms mixing time.

Conformational Analysis and Comparison of NMR and Computational Models. Dihedral angle values as determined from the **8**/HIV-PR complex model are also listed in Table 1. As is apparent, the angles D and G–N correspond well to those estimated by NMR for the solution conformation of (*S*)-**7**. In contrast, the *J* and NOE information surrounding angles A–C and E–F of (*S*)-**7** is incompatible with the conformation for **8** defined in the **8**/HIV-PR complex model. In fact, it appeared impossible to explain the entire set of NMR information in terms of a single conformation for (*S*)-**7** in this region of the molecule. This became particularly

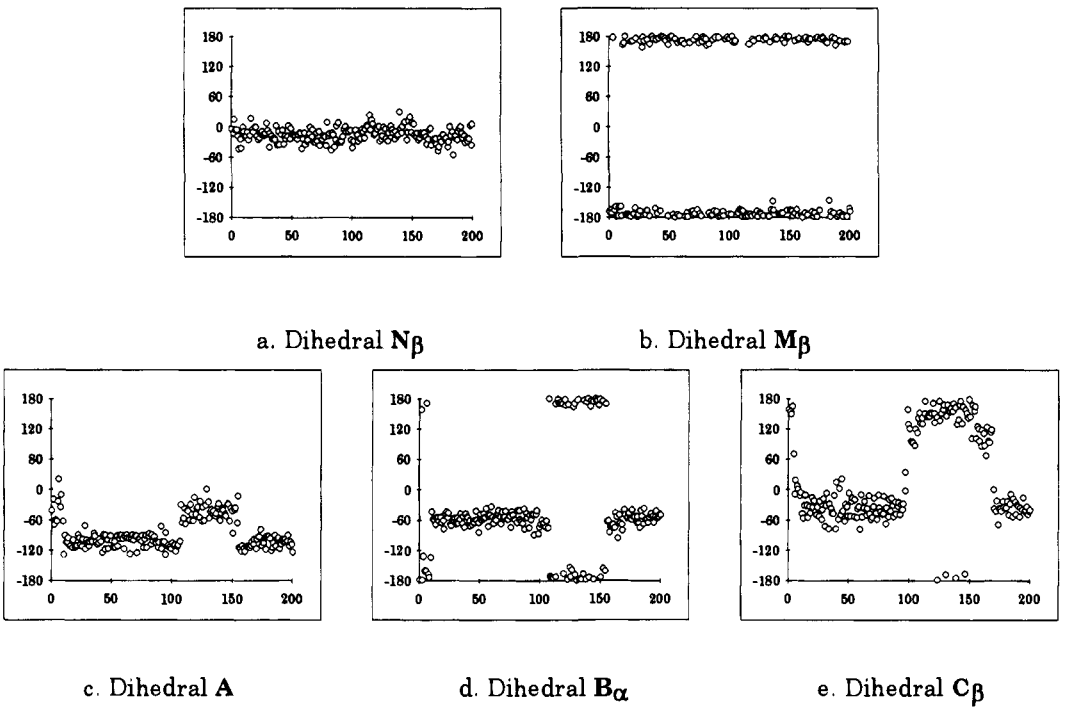

Figure 4. Dihedral angles plotted against frame shots from the MD simulation of uncomplexed ketone **8**. Each frame is equivalent to 0.5 ps. Plots a and b illustrate dihedral angles that remain in one conformational family whereas c–e illustrate dihedral angles involved in a correlated conformational "flip".

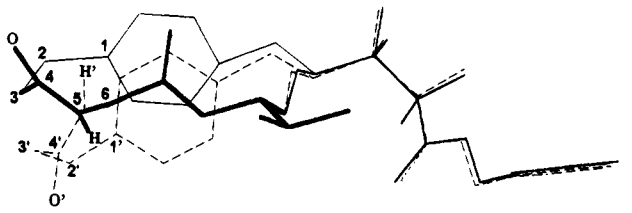

Figure 5. A representation of the major and minor conformers of **8**. The major conformer is represented as a solid line. The minor conformer is represented with a dashed line and designated "primed" numbers. The amide bond formed by atoms 4 and 5 "flips" to the corresponding 4′ and 5. Note that position **5** is the same for both conformers.

obvious when attempting to accommodate unique dihedral angles E compatible with the *J* values found across this bond, as well as the simultaneous occurrence of H-5/H-8 and H-5/H-16 NOEs, with the already established constraints and the remaining NOE information.

To obtain further insight, a short in vacuo MD simulation applied to uncomplexed **8** (100 ps, 300 K) was performed for the purpose of gaining a qualitative understanding of its dynamical behavior. The MD-derived time-averaged dihedral angles are also listed in Table 1. Angles D and G–N are again in good agreement with those derived by NMR for (*S*)-**7** and those found in the **8**/HIV-PR complex model, while angle F corresponds to the NMR estimate for (*S*)-**7**. These angles exist in only one conformational state (see Figure 4a,b). In contrast, angles A–C and E undergo a correlated transition between a major and a minor conformational state during the course of the simulation (see Table 1 and Figure 4c–e).[24] Their relative population of ca. 60:40 translates into an energy difference of roughly 0.25 kcal/mol. A comparison of the two conformers is shown in Figure 5. While the NMR information for this region of (*S*)-**7** is compatible with an average over these two conformational states, the docked inhibitor clearly assumes dihedral angles resembling the *minor* conformation of **8** as defined by the in vacuo simulation.

Conclusions

We have used molecular modeling techniques to design a novel analog of the lead compound 1. The design process was based on a computational model that was found to be consistent with NMR analysis and molecular dynamics. During the course of our work, others have in fact determined the crystal structures of the **1**/HIV-PR and the **8**/HIV-PR complexes.[25] The X-ray structure of **8** as bound in the protease adopts a conformation which is nearly superimposable with that of our model in the regions that are characterizable via NMR and stable via the MD simulations. Furthermore, the torsion angles which are not well-defined by the NMR data and which coincidentally define the two populations of conformations from our MD calculations adopt values *that are exactly intermediate between the values as determined by the MD calculation!* That is, the crystal structure of bound **8** appears to be a time-averaged structure of the "major" and "minor" conformations as defined by MD simulations, thereby lending further verification to the so-called amide plane rotation[24] observed in our molecular dynamics calculations. Such an assertion is supported by larger crystallographic *B* factors of the atoms in this region. Our model has shown that the active site of HIV-PR can accommodate cyclically constrained inhibitors, has prompted the synthetic efforts that culminated in the preparation of macrocyclic ketone **8** that retains biological activity, and has subsequently been verified by X-ray studies. Since the inhibitor may be dissected into a difluorostatone portion and a cyclic portion, design modifications targeting the attributes discussed earlier

can proceed independently on the cyclic portion, which can then be joined to the difluorostatone portion in an efficient, convergent fashion.

Additional Modeling and Predictions. The activity of the cyclic variant **8** tested in this study is slightly lower than that of the acyclic parent inhibitor **1**. Modeling of the cyclically modified inhibitor, however, emphasizes the design flexibility offered by the P_3 linker, which can be any substituted amino acid. Replacement of the glycine with a polar amino acid may increase the water solubility of the inhibitor as well as increase specific interactions with the enzyme. For example, our structural model indicates that an L-asparagine placed in this position may achieve this rather effectively. Additionally, L-asparagine may donate a hydrogen bond to HIV-PR homodimer A aspartic acid no. 8, and accept a hydrogen bond from HIV-PR homodimer B arginine no. 29.

Finally, preliminary in vacuo MD simulations for P_3 variants of **8** demonstrate that the relative populations of the major and minor conformational states may be manipulated. The naturally occurring L-amino acids appear to stabilize the flexible region of the macrocycle toward the *major* (undesired) conformation whereas the D analogs show a greater preponderance of the *minor* (desired) conformer.

While the *minor* conformation (as determined by the in vacuo MD of **8**, see Figure 4) better represents the bound conformation in our computational model, the X-ray structure is inconclusive in this respect. Analogs containing both L- and D-amino acids as the P_3 linker need to be prepared to test these predictions. Future work utilizing the close collaboration of NMR, synthetic, and a priori modeling techniques is continuing in our laboratories to test these predictions.

Experimental Section

Molecular Modeling. All calculations were carried out on a CRAY YMP-2E. Graphics and local manipulations were performed on a Silicon Graphics 4D-380. The molecular modeling analysis was carried out using Insight/Discover.[26] The coordinates of MVT-101 were extracted from the HIV-PR complex, thus creating the active-site cavity. The "bound" conformation of 1 was derived from corresponding backbone atoms of MVT-101.[4] Small van der Waals interactions that occurred between HIV-PR and the inhibitor during the docking procedure were manually eliminated via rotations about single bonds. The hydrated ketone was presumed to create the primary interaction at the active site;[20] the hydroxyl groups were projected toward the catalytic aspartic acid residues. The valine- and α,α-difluoroamido carbonyl groups of 1 (corresponding to Nle and Nle′ carbonyl groups of MVT-101) were aligned to establish the hydrogen bonds with the catalytic water molecule. The complex was then subjected to 50 ps (300 K, 1.0 fs timestep) of molecular dynamics to eliminate small local unfavorable interactions and to assess the qualitative nature of the molecular flexibility of the active site region. The active site was solvated by two concentric shells of water, the origin of which was the center of the active site. The entire system was fully minimized (iterations of 5000 steps of *steepest descents* followed by 10 000 steps of *conjugate gradient* until the maximum derivative was 1.0 kcal/Å), but the MD was applied in the following manner: the innermost shell of water (20 Å radius) was allowed to move about unconstrained during the MD trajectory, while the outer shell of water (5 Å) was fixed to the minimized coordinates with a harmonic potential of 100 000 kcal/mol per Å^2. A distance-dependent dielectric constant of 2.0*R in conjunction with 20 Å cutoffs were used in all molecular dynamics simulations to partially compensate for the lack of explicit water molecules.[27] In our laboratory, we have found that the qualitative behavior of the HIV-PR inhibitors is not dramatically altered by exclusion of explicit water molecules.[28]

General Methods. Melting points were determined on a Thomas-Hoover capillary melting point apparatus and are uncorrected. Silica gel 60 (230-400 mesh ASTM, EM Science) was used for all flash chromatographies. Anhydrous solvents were purchased from Aldrich Chemical Co., Inc. in Sure/Seal bottles. IR spectra were recorded on a Mattson Galaxy 5020 FT-IR spectrophotometer. MS data were collected on Finnigan MAT 4600, MAT TSQ-700, or VG Analytical Limited ZAB2-SE mass spectrometers, and computerized peak matching with perfluorokerosene as a reference was utilized for HRMS. NMR spectra were recorded on Varian Gemini 300, Unity 300, Unity 400, or Unity 500 spectrometers. ^{1}H and ^{13}C NMR signals are reported in ppm from tetramethylsilane, ^{19}F signals are reported in ppm from $CFCl_3$, and coupling constants are reported in hertz (Hz). Combustion analyses were obtained with a Perkin-Elmer Model 2400 elemental analyzer and fell within ±0.4% of the calculated values, except where noted.

[3ξ,4(*S*)]-2,4,5-Trideoxy-4-[[(1,1-dimethylethoxy)carbonyl]amino]-2,2-difluoro-5-(4-hydroxyphenyl)-*N*-(phenylmethyl)-L-*glycero*-pentonamide (3). To a stirred suspension of Pd black (300 mg) in 4.4% HCO_2H/CH_3OH (25 mL) was added ether **2**[1] (6:1 *R/S* ratio, 1.39 g, 2.57 mmol). Additional 300 mg portions of Pd black were added at 0.75, 1.5, and 2.25 h. After 4.25 h total, the catalyst was removed by filtration (CH_3OH rinse), and the filtrate was combined with that from a similar experiment (using 51 mg of ether **2**) and concentrated in vacuo. Recrystallization from cyclohexane/EtOAc gave 1.10 g (92%) of phenol **3** (~6:1 *R/S* ratio) as a fine ivory powder: mp 163–166 °C; IR (KBr) ν_{max} 3412, 3362, 1682, 1545, 1518, 1165 cm^{-1}; ^{1}H NMR (DMSO-d_6) δ 9.18 (nm, 2 H), 7.35–7.2 (m, 5 H), 6.99 (d, 2 H, J = 8.2 Hz), 6.66 (d, 2 H, J = 8.2 Hz), 6.19 (d, 1 H, J = 9.1 Hz), 6.02 (d, 1 H, J = 8.1 Hz), 4.36 (dd, 1 H, J = 15.5, 6.0 Hz), 4.27 (dd, 1 H, J = 15.5, 6.2 Hz), 4.0–3.87 (m, 2 H), 2.64 (m, 2 H), 1.33 (major) and 1.24 (2s, 9 H); ^{19}F NMR (DMSO-d_6) δ major diastereomer: −110.82 (dd, J = 255, 6 Hz), −122.39 (dd, J = 255, 20 Hz), minor diastereomer: −111.05 (dd, J = 255, 6 Hz), −121.78 (dd, J = 255, 21 Hz); mass spectrum *m/z* 479 (M^+ + 29), 451 (M^+ + 1), 423, 379, 352, 351 (100), 333, 243, 91. Anal. ($C_{23}H_{28}F_2N_2O_5$) C, H. N.

In a separate series of experiments in which pure (*S*)-**2** (mp 219–222 °C) was utilized as the starting material, (*S*)-**3** was obtained as white granules: mp 191–192.5 °C; IR (KBr) ν_{max} 3341, 1690, 1547, 1518, 1169 cm^{-1}; ^{1}H NMR (DMSO-d_6) δ 9.17 (~t, 1 H, J = 5.7 Hz), 9.06 (bs, 1 H), 7.36–7.21 (m, 5 H), 6.95 (~d, 2 H, J = 8.4 Hz), 6.61 and 6.56 (2d, 2 H, J = 8.3, 9.1 Hz), 6.19–6.02 (bm), 4.41 (dd, 1 H, J = 15.1, 6.3 Hz), 4.28 (dd, 1 H, J = 15.1, 5.4 Hz), 4.06 (bs, 1 H), 3.77 (m, 1 H), 2.86 (dd [or 2 d], 2 H, J = 14.0, 2.3 Hz), 2.50 (m, 2 H), 1.26 and 1.15 (2s in ~4.6:1 ratio, 9 H); ^{19}F NMR (DMSO-d_6) δ major rotamer: −112.53 (dd, J = 252, 9 Hz), −118.11 (dd, J = 252, 16 Hz), minor rotamer: −113.09 (dd, J = 252, 10 Hz), −117.64 (dd, J = 252, 17 Hz); mass spectrum, *m/z* 479 (M^+ + 29), 451 (M^+ + 1), 423, 395, 379, 352, 351 (100), 333, 91; $[\alpha]^{20}_D$ −22.8° (*c* 0.336, CH_3OH). Anal. ($C_{23}H_{28}F_2N_2O_5$) H, N; C: calcd, 61.32; found, 60.76.

[3ξ,4(*S*)]-2,4,5-Trideoxy-4-[[(1,1-dimethylethoxy)carbonyl]amino]-2,2-difluoro-5-[4-(2-methoxy-2-oxoethoxy)-phenyl]-*N*-(phenylmethyl)-L-*glycero*-pentonamide (4). To a stirred solution of phenol **3** (441 mg, 0.979 mmol) in acetone (6 mL) was added powdered K_2CO_3 (165 mg, 1.20 mmol), $BrCH_2CO_2CH_3$ (110 μL, 1.16 mmol), and a catalytic amount of powdered KI. The flask was stoppered, and stirring was continued for 3 days. The reaction mixture was poured into EtOAc/dilute aqueous NaCl, and the organic layer was separated, washed with dilute aqueous KOH (to remove traces of residual phenol **3**) and brine, and dried ($MgSO_4$). Concentration in vacuo gave 413 mg (81%) of ether **4** as a tacky white solid. In a similar experiment, recrystallization from cyclohexane/EtOAc gave ether **4** (5.5:1 *R/S* ratio) as a white powder: mp 93.5–99.5 °C; IR (KBr) ν_{max} 3352, 1690, 1530, 1512, 1215, 1177 cm^{-1}; ^{1}H NMR ($CDCl_3$) δ 7.38–7.24 (m, 5H), 7.18 (nm, 1 H), 7.10 (d, 2 H, J = 8.6 Hz), 6.81 (d, 2 H, J = 8.6

Hz), 5.00 (d, 1 H, J = 9.2 Hz), 4.72 (nm, 1 H), 4.60 and 4.58 (major) (2s in 1:5.5 ratio, 2 H), 4.50 (dd, 1 H, J = 14.8, 5.7 Hz), 4.42 (dd, 1 H, J = 14.8, 5.7 Hz), 4.1–3.94 (m, 2 H), 3.80 and 3.79 (major) (2s in 1:5.5 ratio, 3H), 3.0–2.8 (m, 2 H), 1.42 and 1.38 (2s, 9 H); ^{19}F NMR ($CDCl_3$) δ minor diastereomer: −113.49 (dd, J = 262, 9 Hz), major diastereomer: −115.83 (dd, J = 262, 9 Hz; other F of minor diastereomer buried under this peak), −120.07 (dd, J = 262, 14 Hz); mass spectrum, m/z 522 (M^+), 495, 451, 423 (100), 405, 243, 223, 91; $[\alpha]^{20}_D$ −33.0° (c 0.81, CH_3OH). Anal. ($C_{26}H_{32}F_2N_2O_7$) H, N; C: calcd, 59.76; found, 59.33.

Pure (*S*)-**4** could not be separated from residual (*S*)-**3** and was therefore utilized without further purification.

[3ξ,4(*S*)]-2,4,5-Trideoxy-4-[[2-[[[[(1,1-dimethylethoxy)carbonyl]amino]acetyl]amino]-3-methyl-1-oxobutyl]amino]-2,2-difluoro-5-[4-(2-methoxy-2-oxoethoxy)phenyl]-*N*-(phenylmethyl)-L-*glycero*-pentonamide (5). A solution of ether **4** (413 mg, 0.790 mmol) in trifluoroacetic acid (TFA) (4 mL) was allowed to stir under nitrogen for 2 h. The solution was concentrated in vacuo and the residue twice dissolved in EtOAc and concentrated again. The resulting TFA salt was dissolved in 1:1 CH_2Cl_2/DMF (3 mL) with stirring under nitrogen, and 1-hydroxybenzotriazole hydrate (HOBT) (128 mg, 0.84 mmol), *N*-methylmorpholine (NMM) (190 μL, 1.73 mmol), Boc-Gly-Val[29] (230 mg, 0.84 mmol), and EDC (168 mg, 0.88 mmol) were added in that order. After 3 days, the mixture was poured into water and extracted twice with EtOAc. The combined extracts were washed with dilute aqueous HCl, $NaHCO_3$, and brine and dried ($MgSO_4$). Concentration in vacuo gave 549 mg of gummy solid which was purified by flash chromatography (3:1 EtOAc/cyclohexane) to give 443 mg (83%) of ester **5** as a white solid. Recrystallization from EtOAc/cyclohexane gave ester **5** (6.6:1 *R*/*S* ratio) as white granules: mp 161–166 °C; IR (KBr) ν_{max} 3395, 3298, 1684, 1647, 1537, 1514, 1206, 1179 cm^{-1}; ^{1}H NMR (DMSO-d_6) δ 9.14 (nm, 1 H), 7.76 (d, 1 H, J = 8.7 Hz), 7.55 (d, 1 H, J = 8.8 Hz), 7.35–7.2 (m, 5 H), 7.13 (d, 2 H, J = 8.6 Hz), 7.09 (m, 1 H), 6.84 (d, 2 H, J = 8.6 Hz), 6.32 (d, 1 H, J = 7.6 Hz), 4.75 (major) and 4.73 (2s in 6.6:1 ratio, 2 H), 4.4–3.93 (m, 5 H), 3.69 (major) and 3.69 (2s, 3 H), 3.56 (inner peaks of apparent AB, 2 H), 2.75 (dd, 1 H, J = 13.4, 8.1 Hz), 2.62 (dd, 1 H, J = 13.4, 6.0 Hz), 1.98 (m, 1 H), 1.38 (major) and 1.36 (2s, 9 H), 0.80 (d, 3 H, J = 6.7 Hz), 0.76 (d, 3 H, J = 6.6 Hz); ^{19}F NMR ($CDCl_3$) δ major diastereomer: −110.67 (d, J = 255 Hz), −122.89 (dd, J = 255, 20 Hz), minor diastereomer: −110.93 (d, J = 257 Hz), −122.29 (dd, J = 257, ~20 Hz); mass spectrum, m/z 707 (M^+ + 29), 679 (M^+ + 1), 623, 579, 405 (100). Anal. ($C_{33}H_{44}F_2N_4O_9$) C, H, N.

Ester (*S*)-**5** was obtained as a white powder after recrystallization from CH_3OH/butanone/EtOAc: mp 209–211 °C; IR (KBr) ν_{max} 3306, 1680, 1653, 1537, 1514, 1211, 1179 cm^{-1}; ^{1}H NMR (DMSO-d_6) δ (major rotamer) 9.25 (t, 1 H, J = 6.0 Hz), 7.94 (d with upfield shoulder, 1 H, J = 8.6 Hz), 7.41–7.21 (m, 6 H), 7.08–7.00 (m, 3 H), 6.77 (d, 2 H, J = 8.4 Hz), 6.25 (bs, 1 H), 4.72 (s, 2 H), 4.36 (m, 2 H), 4.24–3.95 (m, 3 H), 3.69 (s, 3 H), 3.53 (inner peaks of apparent AB, not integrated), 2.94–2.81 (m, 1 H), 2.61 (dd, 1 H, J = 14.1, 10.7 Hz), 1.87 (m, 1 H), 1.38 (2s, 9 H), 0.72 (d, 3 H, J = 7.0 Hz), 0.69 (d, 3 H, J = 7.0 Hz); ^{19}F NMR ($CDCl_3$) δ −109.90 (dd, J = 252, 7 Hz), −119.82 (dd, J = 252, 19 Hz) [shoulders present at δ −109.8 and −119.9]; FAB mass spectrum, m/z 679 (M^+ + 1), 579, 423, 405, 358, 307 (100), 289. Anal. ($C_{33}H_{44}F_2N_4O_9$) C, H, N.

[3ξ,4(*S*)]-2,4,5-Trideoxy-4-[[2-[[[[(1,1-dimethylethoxy)carbonyl]amino]acetyl]amino]-3-methyl-1-oxobutyl]amino]-2,2-difluoro-5-[4-[2-oxo-2-(pentafluorophenoxy)ethoxy]phenyl]-*N*-(phenylmethyl)-L-*glycero*-pentonamide (6). To a stirred suspension of methyl ester **5** (400 mg, 0.589 mmol) in 19:1 CH_3OH/H_2O (20 mL) was added $LiOH·H_2O$ (29 mg, 0.69 mmol). After 2 h, additional $LiOH·H_2O$ (5 mg, 0.81 mmol total) was added, and after an additional 2 h, the solution was concentrated in vacuo. The residue was dissolved in water; the aqueous solution was washed with ether, covered with EtOAc, and acidified with vigorous stirring by the addition of 0.1 N $NaHSO_4$ (10 mL). The organic layer was separated, and the aqueous layer was extracted with a second portion of EtOAc. The combined organic layers were washed with brine and dried ($MgSO_4$). Concentration in vacuo gave 407 mg (392 mg theory) of the corresponding acid, which was dissolved in CH_2Cl_2 (5 mL) and DMSO-d_6 (1 mL). To this stirred solution under nitrogen was added C_6F_5OH (139 mg, 0.755 mmol) and EDC (140 mg, 0.73 mmol). After 3 days the mixture was diluted with water and filtered, washing the ivory solid with water and ether. In this experiment attempted recrystallization from CF_3CH_2OH/EtOAc resulted in partial transesterification to the trifluoroethyl ester. The mixture was thus saponified and reesterified as above to give 394 mg (80%) of crude pentafluorophenyl ester **6**. In a similar experiment, however, recrystallization from CF_3CH_2OH/EtOAc (filtering the hot solution through filter aid) gave pure ester **6** as fine white matted crystals: mp 202–204 °C; IR (KBr) ν_{max} 3389, 2974, 1684, 1653, 1522, 1173, 1121, 1080, 997 cm^{-1}; ^{1}H NMR (DMSO-d_6) δ 9.14 (m, 1 H), 7.77 (d, 1 H, J ~ 9 Hz), 7.54 (d, 1 H, J = 8.9 Hz), 7.35–7.22 (m, 5 H), 7.17 (d, 2 H, J = 8.7 Hz), 7.08 (nm, 1 H), 6.95 (d, 2 H, J = 8.7 Hz), 6.33 (d, 1 H, J = 7.6 Hz), 5.34 (s, 2 H), 4.4–4.18 (m, 4 H), 4.08–3.95 (m, 1 H), 3.55 (nm, 2 H), 2.8–2.58 (m, 2 H), 1.97 (m, 1 H), 1.38 (major) and 1.36 (2s, 9 H total), 0.80 (d, 3 H, J = 6.6 Hz), 0.76 (d, 3 H, J = 6.7 Hz); ^{19}F NMR (DMSO-d_6) δ −110.69 (d, J = 256 Hz), −122.89 (dd, J = 255, 20 Hz), −152.37 (d, J = 20 Hz), −156.95 (t, J = 23 Hz), −161.75 (dd, J = 23, 20 Hz); mass spectrum, m/z 831 (M^+ + 1), 775, 731. Anal. ($C_{38}H_{41}F_7N_4O_9$) C, H, N.

Pentafluorophenylester (*S*)-**6** was not isolated but converted directly to the macrocyclic alcohol (*S*)-**7**.

[9(*S*),12(*S*)]-α,α-Difluoro-β-hydroxy-9-(1-methylethyl)-4,7,10-trioxo-*N*-(phenylmethyl)-2-oxa-5,8,11-triazabicyclo[12.2.2]octadeca-14,16,17-triene-12-propanamide (7). Pentafluorophenyl ester **6** (494 mg, 0.595 mmol) was suspended in 4 N HCl/dioxane (16 mL) with stirring. After 2 h, a clear gel had formed. The solvent and HCl were removed in vacuo, and the residual solid was suspended in dilute aqueous $NaHCO_3/CH_2Cl_2$ with vigorous stirring for 3 days. The mixture was filtered and the ivory solids washed with water and ether. Hot EtOAc was added along with just enough CF_3CH_2OH to dissolve most of the solids; filtration through filter aid and concentration in vacuo gave 256 mg (79%) of macrocyclic alcohol **7**. In a similar experiment the filtrate was concentrated and diluted with hot EtOAc to obtain alcohol (*R*)-**7** as fine white granules: mp >255 °C; IR (KBr) ν_{max} 3412, 3318, 1663, 1537, 1514 cm^{-1}; ^{1}H NMR (DMSO-d_6) δ 9.17 (m, 1 H), 7.90 (m, 1 H), 7.64 (m, 1 H), 7.37–7.2 (m, 5 H), 7.11 (m, 1 H), 7.01 (m, 1 H), 6.93 (m, 1 H), 6.81 (m, 1 H), 6.46 (m, 1 H), 6.14 (dd, 1 H, J = 7.4, 0.9 Hz), 4.60 (d, 1 H, J ~ 15 Hz), 4.5–4.1 (m, 6 H), 3.96 (m, 1 H), 3.72–3.54 (2m, 2 H), 2.76 (m, 1 H), 1.78 (m, 1 H), 0.77–0.71 (m, 6 H); ^{19}F NMR (DMSO-d_6) δ major conformer (85%): −109.96 (dd, J = 256, 5 Hz), −122.71 (dd, J = 256, 20 Hz), minor conformer (15%): −110.45 (d, J = 254 Hz), −122.3 (m); mass spectrum, m/z 547 (M^+ + 1). Anal. ($C_{27}H_{32}F_2N_4O_6·H_2O$) C, H, N.

In the preparation of (*S*)-**7**, the crude material from the deprotection/cyclization was triturated with several portions of boiling CH_3OH to dissolve macrocyclic alcohol (*S*)-**7** and remove some insoluble polymeric material. The solvent was removed in vacuo and the residue triturated with several portions of boiling CF_3CH_2OH. The *insoluble* beige powder was the desired alcohol (*S*)-**7**: mp >245 °C; IR (KBr) ν_{max} 3401, 3298, 1678, 1643, 1543, 1514 cm^{-1}; (see Figure 2 for numbering scheme) ^{1}H NMR (DMSO-d_6) δ 9.26 (H-4″, J = 6.4, 5.8 Hz), 7.89 (H-11, J = 9.9 Hz, $\Delta\delta$/°C[ppb] = −5.3), 7.82 (H-5, J = 7.4, 5.7 Hz, $\Delta\delta$/°C[ppb] = −3.0), 7.34–7.22 (Ph), 7.13 (H-8, J = 8.0 Hz, $\Delta\delta$/°C[ppb] = −3.4), 6.99 (H-18, J = 8.4, 2.0 Hz), 6.92 (H-15, J = 8.4, 2.0 Hz), 6.78 (H-17, J = 8.4, 2.7 Hz), 6.46 (H-16, J = 8.4, 2.7 Hz), 6.31 (OH, J = 7.3 Hz, $\Delta\delta$/°C (ppb) = −5.4), 4.58 (H-3α, J = 15.3 Hz), 4.44 (H-3β, J = 15.3 Hz), 4.41 (H-5″, J = 15.3, 6.4 Hz), 4.31 (H-5″, J = 15.3, 5.8 Hz), 4.30 (H-12, J = 12.1, 9.9, 6.8, 3.5 Hz), 3.98 (H-1″, J = 7.3, 6.8 Hz, $^3J_{H,F}$ = 6.9, 19.8 Hz, $\Delta\delta$/°C (ppb) = −6.0), 3.83 (H-9, J = 8.0, 6.6 Hz), 3.67 (H-6β, J = 13.7, 7.4 Hz), 3.58 (H-6α, J = 13.7, 5.7 Hz), 2.90 (H-13α, J = 13.2, 3.5 Hz), 2.34 (H-13β, J = 13.2, 12.1 Hz), 1.72 (H-1′, J = 6.9, 6.8, 6.6 Hz), 0.72 (H-2′, J = 6.9 Hz), 0.70 (H-3′, J = 6.1 Hz); ^{13}C NMR (DMSO-d_6) δ 168.6 (C-10), 167.7 (C-4), 167.3 (C-7), 163.4 (C-3″), 155.0 (C-1), 138.4, 131.0 (C-17), 130.8 (C-14), 129.9 (C-15), 128.3 (two C), 127.1

(two C), 126.9, 116.7 (C-18), 116.7 (C-2″), 111.5 (C-16), 71.0 (C-1″), 67.1 (C-3), 57.7 (C-9), 49.3 (C-12), 42.9 (C-6), 42.1 (C-5″), 35.5 (C-13), 30.8 (C-1′), 18.5 (C-2′), 18.3 (C-3′); ^{19}F NMR (DMSO-d_6) δ −108.94 (dd, J = 253, 7 Hz), −121.27 (dd, J = 253, 20 Hz); mass spectrum, m/z 575 (M^+ + 29), 547 (M^+ + 1), 113; exact mass calcd for $C_{27}H_{33}F_2N_4O_6$ 547.2368, found 547.2344. Anal. ($C_{27}H_{32}F_2N_4O_6{\cdot}H_2O$) C, H; N: calcd, 9.92; found, 9.50.

[9(*S*),12(*S*)]-α,α-Difluoro-9-(1-methylethyl)-β,4,7,10-tetraoxo-*N*-(phenylmethyl)-2-oxa-5,8,11-tetrabicyclo-[12.2.2]octadeca-14,16,17-triene-12-propanamide (8, MDL 104,168). Alcohol **7** (240 mg, 0.439 mmol) was dissolved in DMSO (6 mL) by heating at 60 °C under nitrogen with vigorous stirring. Upon cooling, the solution was diluted with CH_2Cl_2 (2 mL) and cooled to −15 to −17 °C in an ice/CH_3OH bath; 2 M oxalyl chloride/CH_2Cl_2 (2.0 mL) was added dropwise to give a thin slurry. After 1 h, Et_3N (1.15 mL, 8.25 mmol) was added and the mixture was allowed to slowly warm to room temperature. After 17 h, the mixture was diluted with water/EtOAc. The organic layer was separated and the aqueous layer extracted with a second portion of EtOAc; some insoluble white solid (18 mg) was present which was identified as recovered alcohol **7**. The combined organic extracts were washed three times with water and brine and dried ($MgSO_4$). The crude white solid (101 mg) was purified by flash chromatography (19:1 EtOAc/CH_3OH) to give 27 mg of a nonpolar oil (discarded) and 70 mg of a white solid/gel. Repeated recrystallizations from EtOAc/CF_3CH_2OH gave a white gel which was washed with several portions of 19:1 CH_2Cl_2/CH_3OH. The remaining insoluble gel was recrystallized further from EtOAc/CF_3CH_2OH to give 5 mg of **8** as fine, light beige granules: IR (KBr) ν_{max} 3418, 1667, 1535, 1514 cm^{-1}; ^{19}F NMR (DMSO-d_6) δ −109.12 (d, J = 274 Hz), −111.77 (d, J = 274 Hz), plus minor impurities; mass spectrum (CI, 70 eV), m/z 573 (M^+ + 29), 545 (M^+ + 1), 308 (100), 91; exact mass calcd for $C_{27}H_{31}F_2N_4O_6$ 545.2212, found 545.2230.

In a separate experiment, a suspension of (*S*)-**7** (10.4 mg, 19 μmol) and Dess–Martin periodinane[15] (40 mg, 95 μmol) in CH_3CN (2 mL) was allowed to stir at 25 °C under nitrogen for 4 days. The mixture was diluted with dilute aqueous $NaHCO_3$/$Na_2S_2O_3$ and extracted with EtOAc. The extracts were washed with water and concentrated in vacuo to give 6 mg of a 2:2:1 mixture of recovered (*S*)-**7**/**8**/**8**·H_2O as a white foam: ^{19}F NMR (DMSO-d_6) δ (*S*)-**7**: −108.77 (dd, J = 253, 6 Hz), −121.29 (dd, J = 253, 20 Hz), **8**: −109.17 (d, J = 274 Hz), −111.81 (d, J = 274 Hz), **8**·H_2O: −112.70 (d, J = 254 Hz), −118.05 (d, J = 254 Hz). Addition of H_2O to the sample showed a marked increase in the **8**·H_2O peaks and a marked decrease in the **8** peaks after 1.5 h.

NMR Methods. All NMR data for (*S*)-**7** were obtained from a *ca.* 35 mM solution in DMSO-d_6 on VARIAN Unity-500 and Unity-400 spectrometers and are referenced to internal solvent (^{1}H: δ 2.49; ^{13}C: δ 39.5) and external $CFCl_3$/DMSO-d_6 (^{19}F: δ 0.0), respectively. ^{13}C, ^{19}F, and variable-temperature (25–85 °C) ^{1}H NMR data were obtained on the 400 MHz instrument. Selective DEPT-45 spectra[23] were acquired with a DEPT pulse sequence modified for use of soft rectangular decoupler pulses (PW_{90} = 13.5 ms). Pure absorption mode DQF-COSY,[30] NOESY,[31] and ROESY[32] spectra were acquired at 500 MHz by the hypercomplex method[33] with a spectral width of *ca.* 5000 Hz and an acquisition time of *ca.* 0.2 s in the directly detected dimension ($f2$). Mixing times of 150, 250, 400, 1000 ms (NOESY) and 150 ms (ROESY) were employed, and the spinlock for the ROESY experiment was provided by a train of short (20°) pulses[34] at the carrier frequency with an effective field strength of 4.6 kHz. Approximately 280 (DQF-COSY), 450 (150–400 ms NOESY), 180 (1000 ms NOESY), and 220 (ROESY) complex points were collected in the indirectly detected dimension ($f1$). For all spectra, squared cosine weighting in $f2$, zerofilling in $f1$, and an appropriate gaussian broadening in $f1$ were applied during their transformation into final matrices of 1K × 1K real points.

Enzyme Assay. Recombinant enzyme[17] was partially purified according to Darke.[18] The specific activity of the partially purified protease was in the range of 10–100 units per mg of protein (one unit is defined as the amount of enzyme that will cleave one mmole of Ser-Gln-Asn-Try-Pro-Ile-Val-NH_2 per min at 37 °C under our assay conditions). HIV-1 was assayed against the octapeptide Ser-Gln-Asn-Tyr-Pro-Ile-Val-NH_2. The reaction was performed in 0.1 mL of a buffer containing 0.05 M NaOAc, 0.5 M NaCl, 1 mM EDTA, 0.5% BSA, 5% ethylene glycol, 10% glycerol, pH 5.5. The reaction was stopped after an incubation time of 1 h at 37 °C via quenching with $HClO_4$ (final concentration 0.4M) and centrifuged (Eppendorf) for 5 min. The products of the reaction, Ser-Gln-Asn-Tyr (P_1) and Pro-Ile-Val-NH_2 (P_2), were analyzed by HPLC on a C_{18} column (Ultrasphere ODS, 4.6 × 150 mm, 5 mm, Beckman), by integration of the corresponding peak areas. The elution was performed with an acetonitrile gradient (5% CH_3CN, pH 3.0 to 60% CH_3CN, pH 3.0 in 10 min, at a flow rate of 1 mL/min; retention times: P_1 = 6 min, P_2 = 7 min, and S = 8.3 min). K_i values were determined from a Dixon plot ($1/v$ versus $[I]$).[19] IC_{50} values were also evaluated from a Dixon plot $[S] = K_M$.

Acknowledgment. We thank Gordon J. Madise and Richard L. Hollenbach for computer support during the course of this work. We are indebted to Dr. Jean-Michel Rondeau for sharing his results of the X-ray structure of **8**/HIV-PR prior to publication. Thanks are also due to Dr. Herschel J. R. Weintraub for helpful discussions.

References

(1) (a) Schirlin, D.; Baltzer, S.; Van Dorsselaer, V.; Weber, F.; Weill, C.; Altenburger, J. M.; Neises, B.; Flynn, G.; Remy, J. M.; Tarnus, C. Short and Unexpectedly Potent Difluorostatone Type Inhibitors of HIV-1 Protease. *Biorg. Med. Chem. Lett.* **1993**, *3*, 253–258. (b) Schirlin, D.; Van Dorsselaer, V.; Tarnus, C.; Tyms, A. S.; Baltzer, S.; Weber, F.; Remy, J. M.; Brennan, T.; Farr, R.; Janowick, D. Beneficial Replacement of the P1 Phenylalanine Side Chain in HIV-1 Protease Inhibitors of the Difluorostatone Type. *Biorg. Med. Chem. Lett.* **1994**, *4*, 241–246.

(2) For a review, see: Kessler, H. Conformation and Biological Activity of Cyclic Peptides. *Angew. Chem., Int. Ed. Engl.* **1982**, *21*, 512–523.

(3) Miller, M.; Jaskolski, M.; Rao, J. K. M.; Leis, J.; Wlodawer, A. Crystal Structure of a Retroviral Protease Proves Relationship to Aspartic Protease Family. *Nature* **1989**, *337*, 576–579. PDB reference code 1HVP.

(4) Miller, M.; Schneider, J.; Sathyanarayana, B. K.; Toth, M. V.; Marshall, G. R.; Clawson, L.; Selk, L.; Kent, S. B. H.; Wlodawer, A. Structure of Complex of Synthetic HIV-1 Protease with a Substrate-Base Inhibitor at 2.3 Å Resolution. *Science* **1989**, *246*, 1149–1152. PDB reference code 4HVP.

(5) Swain, A. L.; Miller, M. M.; Green, J.; Rich, D. H.; Schneider, J.; Kent, S. B. H.; Wlodawer, A. X-ray Crystallographic Structure of a Complex Between a Synthetic Protease of Human Immunodeficiency Virus 1 and a Substrate-based Hydroxyethylamine Inhibitor. *Proc. Natl. Acad. Sci. U.S.A.* **1990**, *87*, 8805–8809. PDB reference code 7HVP.

(6) Fitzgerald, P. M. D.; McKeever, B. M.; VanMiddlesworth, J. F.; Springer, J. P.; Heimbach, J. C.; Leu, C. T.; Herber, W, K.; Dixon, R. A. F.; Draker, P. L. Crystallographic Analysis of a Complex Between Human Immunodeficiency Virus Type 1 Protease and Acetyl-Pepstatin at 2.0 Å Resolution. *J. Biol. Chem.* **1990**, *265*, 14209–14219. PDB reference code 5HVP.

(7) (a) Hydroxyethylene based inhibitor: Jaskolski, M.; Miller, M.; Tomasselli, A. G.; Sawyer, T. K.; Staples, D. G.; Heinrikson, R. L.; Schneider, J.; Kent, S. B. H.; Wlodawer, A. Structure at 2.5-Å Resolution of Chemically Synthesized Human Immunodeficiency Virus Type 1 Protease Complexed with a Hydroxyethylene-Based Inhibitor. *Biochemistry* **1991**, *30*, 1600–1609. PDB reference code 8HVP. (b) Symmetric inhibitor: Erickson, J.; Neidhart, D. J.; Van Drie, J.; Kempf, D. J.; Wang, X. C.; Norbeck, D. W.; Plattner, J. J.; Rittenhouse, J. W.; Turon, M.; Wideburg, N.; Kohlbrenner, W. E.; Simmer, R.; Helfrich, R.; Paul, D. A.; Knigge, M. Design, Activity, and 2.8 Å Crystal Structure of a C_2 Symmetric Inhibitor Complexed to HIV-1 Protease. *Science* **1990**, *249*, 527–533. PDB reference 9HVP.

(8) For a current update of other HIV-PR co-crystallization complexes, the Protein Data Bank should be consulted. Protein Data Bank, Chemistry Department, Building 555, Brookhaven National Laboratory, Upton, NY.

(9) Wiley, R. A.; Rich, D. H. Peptidomimetics Derived from Natural Products. *Med. Res. Rev.* **1993**, *3*, 327–384.

(10) Szewczuk, Z.; Rebholz, K. L.; Rich, D. H. Synthesis and Biological Activity of New Conformationally Restricted Analogues of Pepstatin. *Int. J. Peptide Protein Res.* **1992**, *39*, 233–242.

(11) It is important to recognize that experimental verification of our model complexes was not a prerequisite for proposing and synthesizing this macrocycle. In fact, this compound would not have been synthesized in the first place, let alone crystallized, had we not conducted our a priori modeling studies; the model structure of **8**/HIV-PR was the key piece of information that initiated the synthetic efforts. While we were able to verify our model by possessing the crystal structures of both the **1**/HIV-PR and **8**/HIV-PR complexes, the power of the protocol that we have outlined allows a scientific hypothesis to be accurately extended and acted upon well beyond the time period required for its experimental verification to generate new lead compounds.

(12) The stereochemistry of the diastereomeric ethers **2** follows by analogy to the work of (a) Sham, H. L.; Rempel, C. A.; Stein, H.; Cohn, J. Synthesis of 6(S)-Amino-7-cyclohexyl-4,4-difluoro-3(R),5(R)-dihydroxy-2-methylheptane, a Novel Dipeptide Mimic. *J. Chem. Soc., Chem. Commun.* **1990**, 904–905. (b) Thaisrivongs, S.; Pals, D. T.; Kati, W. M.; Turner, S. R.; Thomasco, L. M.; Watt, W. Design and Synthesis of Potent and Specific Renin Inhibitors Containing Difluorostatine, Difluorostatone and Related Analogues. *J. Med. Chem.* **1986**, *29*, 2080–2087. In addition, the (*R*)-diastereomer was converted to lactam *i*, and the relative stereochemistry was confirmed by NOE experiments.

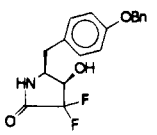

i

(13) El Amin, B.; Anantharamaiah, G. M.; Royer, G. P.; Means, G. E. Removal of Benzyl-type Protecting Groups from Peptides by Catalytic Transfer Hydrogenation with Formic Acid. *J. Org. Chem.* **1979**, *44*, 3442–3444.

(14) Schmidt, U.; Meyer, R.; Leitenberger, V.; Lieberknecht, A.; Griesser, H. The Synthesis of Biphenomycin B. *J. Chem. Soc., Chem. Commun.* **1991**, 275–277.

(15) (a) Dess, D. B.; Martin, J. C. Readily Accessible 12-I-5 Oxidant for the Conversion of Primary and Secondary Alcohols to Aldehydes and Ketones. *J. Org. Chem.* **1983**, *48*, 4155–4156. (b) Dess, D. B.; Martin, J. C. A Useful 12-I-5 Triacetoxyperiodinane (the Dess-Martin Periodinane) for the Selective Oxidation of Primary or Secondary Alcohols and a Variety of Related 12-I-5 Species. *J. Am. Chem. Soc.* **1991**, *113*, 7277–7287. (c) Ireland, R. E.; Lui, L. An Improved Procedure for the Preparation of the Des-Martin Periodinane. *J. Org. Chem.* **1993**, *58*, 2899.

(16) The formation of a single diastereomer in the Dess-Martin oxidation suggests that the relative stereochemistry of **8** is as shown. It has been demonstrated in a similar series of acyclic α,α-difluorostatones that epimerization α to the ketone can generally be avoided. See: Doherty, A. M.; Sircar, I.; Kornberg, B. E.; Quin, J.; Winters, R. T.; Kaltenbronn, J. S.; Jaylor, M. D.; Batley, B. L.; Rapundalo, S. R.; Ryan, M. J.; Painchaud, C. A. Design and Synthesis of Potent, Selective, and Orally Active Fluorine-Containing Renin Inhibitors. *J. Med. Chem.* **1992**, *35*, 2–14.

(17) Guenet, C.; Leppik, R. A.; Pelton, J. T.; Moelling, K.; Lovenberg, W.; Harris, B. A. HIV-1 Protease: Mutagenesis of Asparagine 88 Indicates a Domain Required for Dimer Formation. *Eur. J. Pharmacol.* **1989**, *172*, 443–451.

(18) Darke, P. L.; Leu, C.-T.; Davis, L. J.; Heimback, J. C.; Diehl, R. E.; Hill, W, S.; Dixon, R. A. F.; Sigal, I. S. Human Immunodeficiency Virus Protease. *J. Biol. Chem.* **1989**, *264*, 2307–2312.

(19) Segal, I. H. *Enzyme Kinetics* **1975**, 109.

(20) Gelb, M. H.; Svaren, J. P.; Abeles, R. H. Fluoro Ketone Inhibitors of Hydrolytic Enzymes. *Biochemistry* **1985**, *24*, 1813–1817.

(21) Wüthrich, K. *NMR of Proteins and Nucleic Acids*; John Wiley and Sons, Inc.: New York, 1986.

(22) Malikayil, J. A.; Harbeson, S. A. Conformation of a Neurokinin Antagonist in Solution. *Int. J. Peptide Protein Res.* **1992**, *39*, 497–505, and references therein.

(23) A DEPT-analog of the Selective INEPT experiment: Bax, A. Structure Determination and Spectral Assignment by Pulsed Polarization Transfer via Long-Range ^{1}H-^{13}C Couplings. *J. Magn. Reson.* **1984**, *57*, 314–318. See also: Müller, N.; Bauer, A. Optimized Delays in Heteronuclear Coherehence-Transfer Experiments. *J. Magn. Reson.* **1989**, *82*, 400–405.

(24) A similar dynamical motion has been observed and characterized as an "amide plane rotation". See: Kopple, K. D.; Bean, J. W.; Bhandary, K. K.; Briand, J.; D'Ambrosio, C. A.; Peishoff, C. E. Conformational Mobility in Cyclic Oligopeptides. *Biopolymers* **1993**, *33*, 1093–1099.

(25) Rondeau, J. M.; Tardiff, C. Manuscript in preparation.

(26) Insight/Discover: Biosym Technologies, 10065 Barnes Canyon Road, San Diego, CA 92121.

(27) Weiner, S. J.; Kollman, P. A.; Case, D. A.; Singh, U. C.; Ghio, C.; Alagona, G.; Profeta, S.; Weiner, P. A New Force Field for Molecular Mechanical Simulations of Nucleic Acids and Proteins. *J. Am. Chem. Soc.* **1984**, *106*, 765–784.

(28) Others have also observed little differences between in vacuo calculations and calculations including explicit water molecules for systems of comparable size. For example, see: Matsunaga, T. O.; Collins, N.; Ramaswami, V.; Yamamura, S. H.; O'Brien, D. F.; Hruby, V. Comparison of the Membrane-Bound States of Two Structurally Similar δ-Selective Opioid Peptides by Transferred Nuclear Overhauser Effect Spectroscopy and Molecular Modeling. *Biochemistry* **1993**, *32*, 13180–13189.

(29) Prepared by reaction of Gly-Val (Sigma) with BOC-ON in aqueous THF containing 1 equiv of Et_3N.

(30) (a) Piantini, U.; Sørensen, O. W.; Ernst, R. R. Multiple Quantum Filters for Elucidating NMR Coupling Networks. *J. Am. Chem. Soc.* **1982**, *104*, 6800–6801. (b) Rance, M.; Sørensen, O. W.; Bodenhausen, G.; Wagner, G.; Ernst, R. R.; Wüthrich, K. Improved Spectral Resolution in COSY ^{1}H NMR Spectra of Proteins via Double Quantum Filtering. *Biochem. Biophys. Res. Commun.* **1983**, *117*, 479–485.

(31) Wider, G.; Macura, S.; Kumar, A.; Ernst, R. R.; Wüthrich, K. Homonuclear Two-Dimensional ^{1}H NMR of Proteins. Experimental Procedures. *J. Magn. Reson.* **1984**, *56*, 207–234.

(32) Bothner-By, A. A.; Stephens, R. L.; Lee, J.; Warren, C. D.; Jeanloz, R. W. Structure Determination of a Tetrasaccharide: Transient Nuclear Overhauser Effects in the Rotating Frame. *J. Am. Chem. Soc.* **1984**, *106*, 811–813.

(33) States, D. J.; Haberkorn, R. A.; Ruben, D. J. A Two-Dimensional Nuclear Overhauser Experiment with Pure Absorption Phase in Four Quadrants. *J. Magn. Reson.* **1982**, *48*, 286–292.

(34) Kessler, H.; Griesinger, R. A.; Kerssebaum, R.; Wagner, K.; Ernst, R. R. Separation of Cross-Relaxation and J-Cross-Peaks in 2D Rotating-Frame NMR Spectroscopy. *J. Am. Chem. Soc.* **1987**, *109*, 607–609.